An Additional Structural and Electrical Study of Polymeric Haloplumbates(II) with Heterocyclic Diprotonated Amines

Anna Bonamartini Corradi,[†] Anna Maria Ferrari,*[,†] Lara Righi,[‡] and Paolo Sgarabotto[‡]

Dipartimento di Chimica, Università di Modena e Reggio Emilia, 41100 Modena, Italy, and Dipartimento di Chimica Generale ed Inorganica, Chimica Analitica, Chimica Fisica, Centro di Studio per la Strutturistica Diffrattometrica del CNR, Università di Parma, 43100 Parma, Italy

Received March 23, 2000

The crystal structures of three polymeric bidimensional piperazinium, *N*,*N*′-dimethylpiperazinium, and *N*-benzylpiperazinium hydrate haloplumbates(II) and one polymeric monodimensional *N*,*N*′-dimethylpiperazinium hydrate haloplumbate(II) were determined by means of X-ray analysis. The $(pipzH_2)[PbCl_4]$ salt is monoclinic, space group $P2_1/c$, with $a = 5.778(2)$ Å, $b = 22.612(26)$ Å, $c = 9.061(4)$ Å, $\beta = 95.37(6)°$, $Z = 4$; $(me_2pipzH_2)[PbBr_4]$ crystallizes in the monoclinic $P2_1$ space group with $a = 6.101(3)$ Å, $b = 18.822(12)$ Å, $c = 6.229(2)$ Å, $\beta = 98.62(4)°$, $Z = 2$; the crystals of $(me_2pipzH_2)_2[Pb_3I_{10}]\cdot 4H_2O$ are monoclinic, space group $P2_1/c$, $a = 19.054(4)$ Å, $b = 12.239(3)$ Å, $c = 18.273(4)$ Å, $\beta = 93.42(12)°$, $Z = 4$; $(benzpipzH_2)_3[Pb_2Br_{10}]\cdot 2H_2O$ crystallizes in the monoclinic $P2_1/c$ space group with $a = 22.380(22)$ Å, $b = 9.304(15)$ Å, $c = 24.577(25)$ Å, $\beta = 94.28(11)°$, $Z = 2$. Different model type structures, such as one-dimensional linear chain, ribbonlike, and perovskite-like, were observed, and factors governing these structural arrangements are pointed out. The compounds were also investigated by means of thermal and electrical measurements, and correlations between electrical properties and crystal structures were noted.

Introduction

For an element as familiar and widely used as lead, remarkably little is known of its coordination chemistry. Perhaps because of its size and high X-ray absorption, even less is known of its structural chemistry. For lead(II) the available structures are sporadic and diverse, exhibiting a wide variety of coordination numbers and stereochemistries with or without the suggestion of a "lone pair" in the coordination sphere.[1] Much effort has been devoted to the investigation of construction strategies for studying different structural archetypes developed by haloplumbate(II) systems in order to highlight all the factors controlling both stereochemistry and correlations between symmetry and thermal and electrical properties.

To date, we have pointed out the structural differences and the thermal and electrical properties of haloplumbate(II) systems obtained by using monoprotonated heterocyclic amines and diprotonated linear amines.[2,3] The aim of this work is to provide a deeper knowledge of the polymeric nature of the controlling factor of haloplumbates(II) and to explore the possible formation of new solid inorganic/organic composites presenting unusual properties.

In particular, we present the results of a study on the synthesis and structural and electrical characterization of mono- and bidimensional haloplumbate(II) systems having as counterions diprotonated heterocyclic amines such as piperazine, *N*,*N*′-dimethylpiperazine, and *N*-benzylpiperazine.

Attention has been focused on obtaining information on the polymeric inorganic anions of the synthesized complexes, while the organic counterions have been considered with respect to their steric hindrance and to their hydrogen-bonding capability responsible for the molecular network.

Experimental Section

Synthesis. Piperazinium Tetrachloroplumbate(II). The crystalline compound was prepared by dissolving a 1:1 molar mixture of piperazine and $PbCl_2$ in a concentrated hydrogen chloride solution (HCl (37%)) and allowing the solution to stand for several hours at room temperature. Slow evaporation enabled the formation of white lamellar crystals, suitable for X-ray single-crystal analysis. Elemental anal. Found for $(pipzH_2)[PbCl_4]$ (compound **1**): C, 11.00; H, 2.80; N, 6.40. Calcd for $C_4H_{12}PbCl_4N_2$: C, 10.99; H, 2.77; N, 6.41.

***N*,*N*′-Dimethylpiperazinium Haloplumbates(II).** The compounds $(me_2pipzH_2)[PbBr_4]$ and $(me_2pipzH_2)_2[Pb_3I_{10}]\cdot 4H_2O$ were precipitated by mixing concentrated hydrogen halide solutions (HBr (40%) and HI (57%)) of the *N*,*N*′-dimethylpiperazine and PbX_2 (X = Br, I) in a 1:1 stoichiometric molar ratio. By slow evaporation of the solutions, white needle crystals for the bromide and yellow acicular crystals for the iodide were synthesized. Elemental anal. Found for $(me_2pipzH_2)[PbBr_4]$ (compound **2**): C, 11.19; H, 2.50; N, 4.35. Calcd for $C_6H_{16}PbBr_4N_2$: C, 11.21; H, 2.51; N, 4.36.

Elemental anal. Found for $(me_2pipzH_2)_2[Pb_3I_{10}]\cdot 4H_2O$ (compound **3**): C, 6.60; H, 1.85; N, 2.54. Calcd for $C_{12}H_{40}Pb_3I_{10}N_4O_4$: C, 6.57; H, 1.84; N, 2.55.

***N*-Benzylpiperazinium Bromoplumbate(II).** The compound was separated by mixing an equal molar mixture of the diprotonated amine and $PbBr_2$ in a concentrated hydrogen bromide solution (40%) and allowing the solution to stand for some hours. The product crystallizes in white acicular single crystals. Elemental anal. Found for $(benzpipzH_2)_3[Pb_2Br_{10}]\cdot 2H_2O$ (compound **4**): C, 22.19; H, 3.26; N, 4.70. Calcd for $C_{33}H_{58}Pb_2Br_{10}N_6O_2$: C, 22.21; H, 3.28; N, 4.71.

Crystal Structure Determination. Intensity data for compounds **1**, **2**, **3**, and **4** were collected by mounting crystals on the diffractometer

[†] Università di Modena e Reggio Emilia.
[‡] Università di Parma.

(1) Engelhardt, L. M.; Patrick, J. M.; Whitaker, C. R.; White, A. H. *Aust. J. Chem.* **1987**, *40*, 2107.
(2) Bonamartini Corradi, A.; Bruni, S.; Cariati, F.; Ferrari A. M.; Saccani, A.; Sandrolini, F.; Sgarabotto, P. *Inorg. Chim. Acta* **1997**, *254*, 137.
(3) Bonamartini Corradi, A.; Ferrari A. M.; Pellacani, G. C.; Saccani, A.; Sandrolini, F.; Sgarabotto, P. *Inorg. Chem.* **1999**, *38*, 716.

10.1021/ic000319k CCC: $20.00
Published on Web 12/15/2000

Table 1. Experimental Data for the Crystallographic Analysis of Compounds **1**−**4**

	1	**2**	**3**	**4**
chemical formula	$C_4H_{12}Cl_4N_2Pb$	$C_6H_{16}Br_4N_2Pb$	$C_{12}H_{40}I_{10}N_4O_4Pb$	$C_{33}H_{58}Br_{10}N_6O_2Pb_2$
fw	437.2	643.0	2195.1	1784.3
space group	$P2_1/c$ (No. 14)	$P2_1$ (No. 4)	$P2_1/c$ (No. 14)	$P2_1/c$ (No. 14)
a, Å	5.778(2)	6.101(3)	19.054(4)	22.380(22)
b, Å	22.612(26)	18.822(12)	12.239(3)	9.304(15)
c, Å	9.061(4)	6.229(2)	18.273(4)	24.577(25)
α, deg	90	90	90	90
β, deg	95.37(6)	98.62(4)	93.42(12)	94.28(11)
γ, deg	90	90	90	90
V, Å^3	1178.6(15)	707.3(9)	4253.8(17)	5103.9(18)
Z	4	2	4	4
ρ_{calc}, g cm^{-3}	2.46	3.02	3.43	2.32
ρ_{obs}, g cm^{-3}	2.45	3.00	3.41	2.31
T, °C	20	20	20	20
μ, cm^{-1}	151.7	231.9	191.2	144.5
λ, Å	0.710688	0.710688	0.710688	0.710688
R^a	0.052	0.029	0.054	0.030
$R_w{}^b$	0.054	0.031	0.055	0.032

[a] $R = \sum|\Delta F|/\sum|F_o|$. [b] $R_w = [\sum w(\Delta F^2)^2/\sum w(F_o^2)^2]^{1/2}$.

in a random orientation; the resulting crystal data with other details regarding data collection and refinements are noted in Table 1. The structures were solved by the heavy-atom method, and refinements were carried out by full-matrix least-squares and anisotropic thermal parameters for non-hydrogen atoms; hydrogens were placed in the calculated positions and introduced in the last refinement cycle. The intensities I_{hkl}, determined by the Lehmann and Larsen procedure, were corrected for Lorentz and polarization effects and put on an absolute scale by least-squares; an absorption correction (Walker and Stuart method, min, max correction 0.94−1.10) was also applied.[4,5] The atomic scattering factors for the neutral atoms were taken from the *International Tables for X-Ray Crystallography*.[6] All the calculations were carried out on the GOULD 4040 POWER NODE computer of the Centro di Studio per la Strutturistica Diffrattometrica del CNR, Parma using SHELX76, SHELX86, PARST, ABSORB, and ORTEP programs.[7−11]

Electrical Measurements. Fine powders, obtained by grinding crystals of the **1** and **2** compounds, were compacted under a pressure of 50 N/mm^2 into the shape of disks 28 mm in diameter and up to 2 mm in thickness. Samples were then coated with gold by evaporation under vacuum providing a three-terminal electrode configuration which has been proved to be the most suitable for these materials. Prior to any electrical measurements, samples were sintered in dry nitrogen for 8 h at 383 K. A three-terminal technique was used for both direct (dc) and alternating current (ac) measurements owing to the rather low electrical conductivity exhibited by these compounds at room temperature. The voltmeter−ammeter method in dc and the Schering-bridge method in ac measurements (2×10^{-1} to 1×10^5 Hz) were used with cells and instrumentation according to ASTM D257 and D150 standards, respectively. All measurements were made in dry nitrogen to avoid any possible contamination by gases or vapors on the surfaces of the samples. X-ray diffraction analysis was lastly performed in order to determine possible structural changes occurring in the samples during the electrical investigations.

On account of their extreme instability shown after compression, electrical and dielectrical measurements on $(me_2pipzH_2)_2[Pb_3I_{10}]\cdot 4H_2O$ and $(benzpipzH_2)_3[Pb_2Br_{10}]\cdot 2H_2O$ were not carried out.

(4) Lehmann M. S.; Larsen F. K. *Acta Crystallogr., Sect. A* **1974**, *30*, 580.
(5) Walker, M.; Stuart, D. *Acta Crystallogr. A* **1983**, *39*, 158.
(6) *International Tables for X-Ray Crystallography*; Kynoch Press: Birmingham, 1974; Vol. IV.
(7) Sheldrick, G. *SHELX76, Program System for Crystal Structure Determination*; University of Cambridge: Cambridge, 1976.
(8) Sheldrick, G. *SHELX86, Program for the Solution of Crystal Structure*; University of Göttingen: Göttingen, FRG, 1986.
(9) Nardelli, M. *Comput. Chem.* **1983**, *7*, 95.
(10) Ugozzoli, F. *ABSORB, a program for Walker and Stuart's absorption correction*; University of Parma: Parma, 1983.
(11) Johnson, C. K. ORTEP. Technical Report ORNL-3794; Oak Ridge National Laboratory: Oak Ridge, TN, 1965.

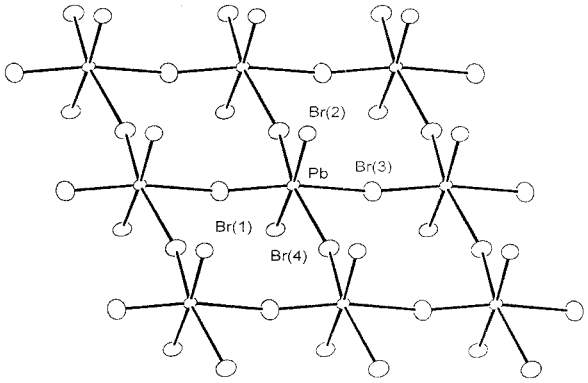

Figure 1. Perspective view of inorganic layers in the perovskite-like structure of $(me_2pipzH_2)[PbBr_4]$ (**2**) with vibrational ellipsoids at the 50% probability level.

Physical Measurements. Thermogravimetric and differential scanning calorimetric analysis were performed with a TA instrument DSC10 system equipped with a mechanical cooler and an automatic data acquisition and computer system TA2000. Carbon, hydrogen, and nitrogen were analyzed with a Carlo Erba model 1106 elemental analyzer.

Results and Discussion

The crystal structures of the four synthesized compounds show distinctly different structural arrangements. Of particular interest is the observation that chemically similar ligands can produce dramatic changes in the stereochemistry due to the differences in hydrogen-bonding capabilities of the cations as well as to differences in packing energies. This study reveals a rich variety of coordination structural archetypes including two-dimensional, layered structures, ribbon-like structures, and strictly monodimensional structures.

Crystal Structure of $(me_2pipzH_2)[PbBr_4]$. Compound 2. The structure of the $(me_2pipzH_2)[PbBr_4]$ salt consists of infinite two-dimensional layers of $PbBr_6$ units, which lie in the *xz* plane, with dimethylpiperazinium dications situated between the sheets (Figures 1 and 2). Each Pb(II) atom is surrounded by six bromide atoms in a slightly distorted octahedral arrangement in which the bridging bromide atoms identify the equatorial plane and the terminal ones are in the axial positions. Bond distances and angles, reported in Table 2, are in good agreement with those previously found in other haloplumbate(II) systems with perovskite-like structure. $PbBr_6$ corner-sharing octahedra

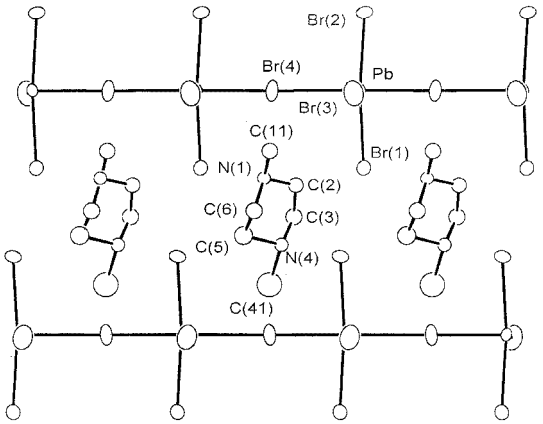

Figure 2. Projection of the structure of $(me_2pipzH_2)[PbBr_4]$ (**2**) along the *z* direction with vibrational ellipsoids at the 50% probability level.

Table 2. Bond Distances (Å) and Angles (deg) with Esd's in Parentheses Involving the Inorganic Moieties of Compounds **1** and **2**

	1 X = Cl	**2** X = Br
Pb−X(1)	2.843(5)	2.980(6)
Pb−X(2)	2.791(6)	3.025(6)
Pb−X(3)	2.891(4)	2.954(2)
Pb−X(4)	2.884(8)	2.837(2)
Pb−X(3)^{i}	2.894(4)	3.164(2)
Pb−X(4)^{i}	2.916(8)	3.431(2)
X(1)−Pb−X(2)	89.3(2)	173.8(2)
X(1)−Pb−X(3)	88.4(1)	89.2(2)
X(1)−Pb−X(4)	169.3(2)	86.4(2)
X(1)−Pb−X(3)^{i}	87.8(1)	89.3(2)
X(1)−Pb−X(4)^{ii}	86.9(2)	92.7(1)
X(2)−Pb−X(3)	87.5(1)	89.9(2)
X(2)−Pb−X(4)	81.2(2)	87.6(2)
X(2)−Pb−X(3)^{i}	88.4(1)	92.5(2)
X(2)−Pb−X(4)^{ii}	174.2(2)	93.5(2)
X(3)−Pb−X(4)	96.0(2)	92.8(1)
X(3)−Pb−X(3)^{i}	174.4(1)	171.4(1)
X(3)−Pb−X(4)^{ii}	88.0(2)	100.1(1)
X(4)−Pb−X(3)^{i}	87.1(2)	95.6(1)
X(4)−Pb−X(4)^{ii}	103.0(2)	167.1(1)
X(3)^{i}−Pb−X(4)^{ii}	95.8(2)	71.5(1)
i	$1 + x, y, z$	$1 + x, y, z$
ii	$x, {}^1/_2 - y, {}^1/_2 + z$	$x, y, z - 1$

show four Pb−Br shorter distances ranging from 2.837(2) to 3.025(6) Å and two longer Pb(1)−Br(2) ($1 + x, y, z$) (3.164(2) Å) and Pb(1)−Br(4) ($x, y, z - 1$) (3.431(2) Å) ones. Consequently, the halogen bridges are asymmetric but almost perfectly linear as confirmed by the Pb(1)−Br(4)−Pb(1) (167.0°) and Pb(1)−Br(2)−Pb(1) (171.4°) angles.

The minimum Pb···Pb ($x - 1, y, z$) intralayer distance, corresponding to the *a* lattice constant, and the Pb···Pb ($-x, y - {}^1/_2, -z$) interlayer distances are 6.10 and 9.58 Å, respectively. The latter value is considerably smaller than the ones previously found in $(2meptH_2)[PbX_4]$ (X = Cl, Br) of 12.15 and 12.7 Å respectively for chloride and bromide compounds.[3] This variation marks the role of the diverse diamine spacers used which, due to their different size, create a modulation between the inorganic layers.

It is worth noting that Pb atoms belonging to adjacent layers are not perfectly overlapped but shifted by about 11°. This remarkable displacement can be explained by considering the steric hindrance of the CH_3 groups, directed toward the empty interlayer space, which are responsible for the repulsive effect on adjacent ammonium dications. Packing is determined by van der Waals interactions as well as hydrogen bonds involving nitrogen atoms of the organic moieties and the unique terminal bromide atoms of the layers; N(4)···Br(3) ($1 - x, {}^1/_2 + y, 1 - z$) 3.28(1) Å, N(1)···Br(1) 3.34(2) Å.

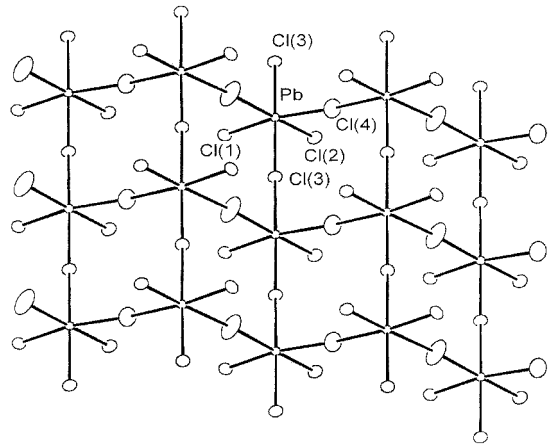

Figure 3. Perspective view of inorganic layers in the perovkite-like structure of $(pipzH_2)[PbCl_4]$ (**1**) with vibrational ellipsoids at the 50% probability level.

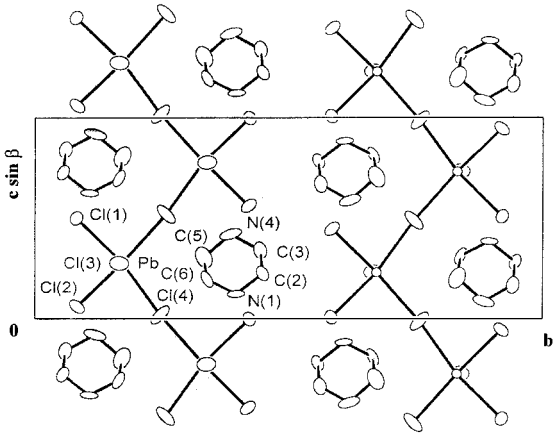

Figure 4. Projection of the structure of $(pipzH_2)[PbCl_4]$ (**1**) along the *x* direction with vibrational ellipsoids at the 50% probability level.

Crystal Structure of $(pipzH_2)[PbCl_4]$. Compound 1. The piperazinium compound presents a similar arrangement with respect to the above-described dimethylpiperazinium one. The crystal structure consists of layers of $[PbCl_4]_n^{2-}$ anions and organic dications (Figures 3 and 4). The ($PbCl_6$) corner-sharing octahedra are joined by symmetrically and linearly bridging chlorine atoms, as also confirmed by Pb−Cl(3)−Pb and Pb−Cl(4)−Pb angles of 174°.

The structure contains corrugated inorganic layers piled along the *y* axis. A remarkable dissimilarity is noted between the present compound and the dimethylpiperazinium one, deriving both from the different Pb···Pb intralayer distances (Pb···Pb ($x - 1, y, z$) 5.78 Å, Pb···Pb ($x, {}^1/_2 - y, z - {}^1/_2$) 5.80 Å, Pb···Pb ($x - 1, y - {}^1/_2, z + {}^1/_2$) 8.48 Å, Pb···Pb ($1 + x, {}^1/_2 - y, z + {}^1/_2$) 7.88 Å) and from the interlayer distances (Pb···Pb ($-x, -y, -z$) 9.36 Å), slightly shorter than those observed in the $(me_2pipzH_2)[PbBr_4]$ complex (Table 2). In fact, the absence of CH_3 groups guarantees a dense structural arrangement where the organic cations reside within the troughs of this corrugated structure, in which they are held by hydrogen bonds involving two different chlorine atoms belonging to a common layer (N(1)···Cl(1) ($1 + x, {}^1/_2 - y, z - {}^1/_2$) 3.15(2) Å, N(4)···Cl(2) ($1 + x, {}^1/_2 - y, z + {}^1/_2$) 3.22(2) Å). The formation of a perovskite-like structure has been previously obtained for other polymeric

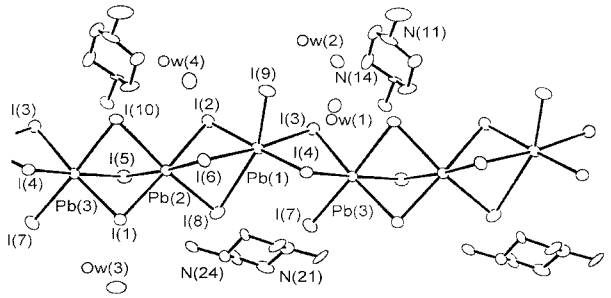

Figure 5. Perspective view of $(me_2pipzH_2)_2[Pb_3I_{10}]\cdot 4H_2O$ (**3**) showing the chain arrangement of the structure with vibrational ellipsoids at the 50% probability level.

bidimensional haloplumbates(II), but till now this structural motif has been observed only in few cases.[12,13] This arrangement is responsible for the novel situation whereby the nonbridging chlorine atoms, engaged in the hydrogen bonding, on each lead have a cis rather than the usual trans relationship. In a sense, the structure can be viewed as a layered lattice in which both the anions and cations are part of each layer, the layers then being held together by van der Waals interactions.

Crystal Structure of $(me_2pipzH_2)_2[Pb_3I_{10}]\cdot 4H_2O$. Compound 3. The bulk structural archetype of this compound is closely similar to what has been observed in $(2meptH_2)[Pb_{1.5}I_5]$ and $(mepnH_2)_2[Cd_3Cl_{10}]$.[3,14] The striking feature of the $(me_2pipzH_2)_2[Pb_3I_{10}]\cdot 4H_2O$ structure is the 1-D polymeric endless chains, running along the *y* axis, of $[Pb_3I_{10}^{4-}]_n$ trimeric units which are connected by shared edges (Figure 5, Table 3). Furthermore, the structure revealed uncoordinated water molecules and dimethylpiperazinium dications anchoring two adjacent chains through hydrogen-bonding interactions. In each trimeric unit, three crystallographically independent Pb atoms are present. Pb(2) is surrounded by six bridging halide atoms, which enable the metal ion to be connected to Pb(1) and Pb(3). The octahedra are joined by two triangular faces (I(1), I(5), I(10) and I(2), I(6), I(8)), while adjacent trimers share edges (I(3) and I(4)). In this case, the observed linear structural development is determined especially by the presence of water molecules involving terminal and bridging iodine atoms (I(9)···O(4) 3.45(1) Å, O(4)···I(9) ($-x$, $^1/_2 + y$, $^1/_2 - z$) 3.42(2) Å, O(3)···I(7) ($1 - x$, $y - ^1/_2$, $^1/_2 - z$) 3.42(2) Å, O(2)···I(9) (x, $1 + y$, z) 3.72(2) Å, O(3)···I(8) ($1 - x$, $y + ^1/_2$, $^1/_2 - z$) 3.77(3) Å) in hydrogen bonds, which are competitive with respect to those implying, in the similar $(2meptH_2)[Pb_{1.5}I_5]$ and $(mepnH_2)_2[Cd_3Cl_{10}]$ compounds, the nitrogen amine atoms. The I(8) involvement in a hydrogen bond might justify the remarkable Pb(1)−I(8) distance of 3.675(3) Å that is longer than those found in the present compound and longer than the ones observed in the closely similar $(2meptH_2)[Pb_{1.5}I_5]$ haloplumbate.[3] However, a Pb−I distance of 3.882 Å has been found in the elsewhere reported $[CH_3SC(=NH_2)NH_2]_3PbI_5$ compound, which shows alternating short and long Pb−I bond lengths down the PbI_5^{3-} chains.[15] It is worth considering that the presence of uncoordinated water molecules and the use of an organic cation having a higher steric hindrance give rise to a greater structural density with respect to the above cited methylpentanediamine and methylpropanediamine compounds. The structure is tridimensionally built up of a network of hydrogen-bonding interactions: N(14)···O(1) (x, $^3/_2 - y$, $^1/_2 + z$) 2.86(3) Å, N(24)···O(3) ($1 - x$, $1 - y$, $-z$) 2.71(3) Å, O(2)···I(3) (x, $1 + y$, z) 3.69(2) Å, O(1)···I(4) (x, $1 + y$, z) 3.61(2) Å, O(1)···O(4) ($-x$, $^1/_2 + y$, $^1/_2 - z$) 2.86(2) Å, O(5)···I(3) (x, $^2/_3 - y$, $z - ^1/_2$) 3.46(3) Å, I(4)···N(21) 3.54(3) Å, N(11)···O(2) 2.78(1) Å.

Table 3. Bond Distances (Å) and Angles (deg) with Esd's in Parentheses Involving the Inorganic Moiety of Compound **3**[a]

Pb(1)−I(2)	3.184(3)	Pb(2)−I(6)	3.180(3)
Pb(1)−I(3)	3.278(3)	Pb(2)−I(8)	3.071(3)
Pb(1)−I(4)	3.332(3)	Pb(2)−I(10)	3.355(3)
Pb(1)−I(6)	3.256(3)	Pb(3)−I(1)	3.254(3)
Pb(1)−I(8)	3.675(3)	Pb(3)−I(3)^i	3.279(3)
Pb(1)−I(9)	2.978(3)	Pb(3)−I(4)^i	3.303(3)
Pb(2)−I(1)	3.226(3)	Pb(3)−I(5)	3.246(3)
Pb(2)−I(2)	3.245(3)	Pb(3)−I(7)	3.065(3)
Pb(2)−I(5)	3.273(3)	Pb(3)−I(10)	3.330(3)
I(2)−Pb(1)−I(3)	91.8(1)	I(6)−Pb(2)−I(8)	86.2(1)
I(2)−Pb(1)−I(4)	173.2(1)	I(6)−Pb(2)−I(10)	90.7(1)
I(2)−Pb(1)−I(6)	87.9(1)	I(8)−Pb(2)−I(10)	173.4(1)
I(2)−Pb(1)−I(8)	76.2(1)	I(1)−Pb(3)−I(3)^i	173.8(1)
I(2)−Pb(1)−I(9)	89.7(1)	I(1)−Pb(3)−I(4)^i	93.1(1)
I(3)−Pb(1)−I(4)	92.0(1)	I(1)−Pb(3)−I(5)	84.1(1)
I(3)−Pb(1)−I(6)	173.2(1)	I(1)−Pb(3)−I(7)	93.4(1)
I(3)−Pb(1)−I(8)	110.8(1)	I(1)−Pb(3)−I(10)	88.9(1)
I(3)−Pb(1)−I(9)	85.6(1)	I(3)^i−Pb(3)−I(4)^i	92.5(1)
I(4)−Pb(1)−I(6)	87.7(1)	I(3)^i−Pb(3)−I(5)	90.1(1)
I(4)−Pb(1)−I(8)	107.7(1)	I(3)^i−Pb(3)−I(7)	89.5(1)
I(4)−Pb(1)−I(9)	84.9(1)	I(3)^i−Pb(3)−I(10)	88.6(1)
I(6)−Pb(1)−I(8)	75.8(1)	I(4)^i−Pb(3)−I(5)	175.5(1)
I(6)−Pb(1)−I(9)	87.6(1)	I(4)^i−Pb(3)−I(7)	85.7(1)
I(8)−Pb(1)−I(9)	158.4(1)	I(4)^i−Pb(3)−I(10)	90.4(1)
I(1)−Pb(2)−I(2)	175.1(1)	I(5)−Pb(3)−I(7)	98.0(1)
I(1)−Pb(2)−I(5)	84.2(1)	I(5)−Pb(3)−I(10)	86.0(1)
I(1)−Pb(2)−I(6)	96.5(1)	I(7)−Pb(3)−I(10)	175.6(1)
I(1)−Pb(2)−I(8)	97.2(1)	Pb(2)−I(1)−Pb(3)	76.9(1)
I(1)−Pb(2)−I(10)	88.9(1)	Pb(1)−I(2)−Pb(2)	81.4(1)
I(2)−Pb(2)−I(5)	91.1(1)	Pb(1)^i−I(3)^i−Pb(3)	83.9(1)
I(2)−Pb(2)−I(6)	88.2(1)	Pb(1)^i−I(4)^i−Pb(3)	82.6(1)
I(2)−Pb(2)−I(8)	84.6(1)	Pb(2)−I(5)−Pb(3)	76.4(1)
I(2)−Pb(2)−I(10)	89.5(1)	Pb(1)−I(6)−Pb(2)	81.2(1)
I(5)−Pb(2)−I(6)	175.8(1)	Pb(1)−I(8)−Pb(2)	76.2(1)
I(5)−Pb(2)−I(8)	97.9(1)	Pb(2)−I(10)−Pb(3)	74.1(1)
I(5)−Pb(2)−I(10)	85.2(1)		

[a] i = x, $1 + y$, z.

Metal−metal contacts between independent intratrimer atoms Pb(1)···Pb(2) 4.19 Å and Pb(2)···Pb(3) 4.03 Å are shorter than those connecting the trimers Pb(1)···Pb(3) (x, $1 + y$, z) 4.38(5) Å. In addition, in the octahedra, the Pb−I distances between terminal iodine atoms Pb(1)−I(9) and Pb(3)−I(7) are 2.978(3) and 3.065(3) Å, respectively, while those involving bridging iodine ones vary from 3.071(3) Å to 3.355(3) Å excluding the above-reported Pb(1)−I(8). The equatorial angles vary in the 84.2−97.9° interval for Pb(2) and in the ranges 84.1−98.0° and 85.6−91.8° for Pb(1) and Pb(3), respectively, indicating slightly distorted octahedral arrangements. Intermolecular Pb···Pb distances are 10.35 Å, while intramolecular ones, corresponding to the *b* axis, are 12.24 Å.

Crystal Structure of $(benzpipzH_2)_3[Pb_2Br_{10}]\cdot 2H_2O$. Compound 4. While strictly monodimensional and two-dimensional layer compounds have been often synthesized and the correlations between their structures and properties satisfactorily rationalized, those of ribbonlike structures are less well understood, probably due to the fact that till now very few compounds presenting this structural motif have been isolated.[3,16] The salt of the *N*-benzyl derivative contains discrete organic dications, uncoordinated water molecules and inorganic ribbons (Figures

(12) Mitzi, D. B.; Wang, S.; Feild, A.; Chess, C. A.; Guloy, A. M. *Science* **1995**, *267*, 1473.
(13) Mitzi, D. B. *Prog. Inorg. Chem.* **1999**, *48*, 1.
(14) Bonamartini Corradi, A.; Bruckner, S.; Cramarossa, M. R.; Manfredini, T.; Menabue, L.; Saladini, M.; Saccani, A.; Sandrolini, F.; Giusti, J. *Chem. Mater*. **1993**, *5*, 90.
(15) Mousdis, G. A.; Gionis, V.; Papavassiliou, G. C.; Raptopoulou, C. P.; Terzis, A. *J. Mater. Chem.* **1998**, *8*, 2259.

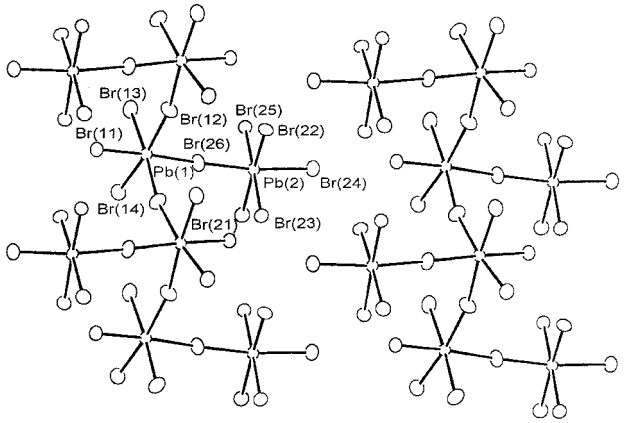

Figure 6. Perspective view of $(benzpipzH_2)_3[Pb_2Br_{10}]\cdot 2H_2O$ (**4**) showing the ribbon arrangement of the structure with vibrational ellipsoids at the 50% probability level.

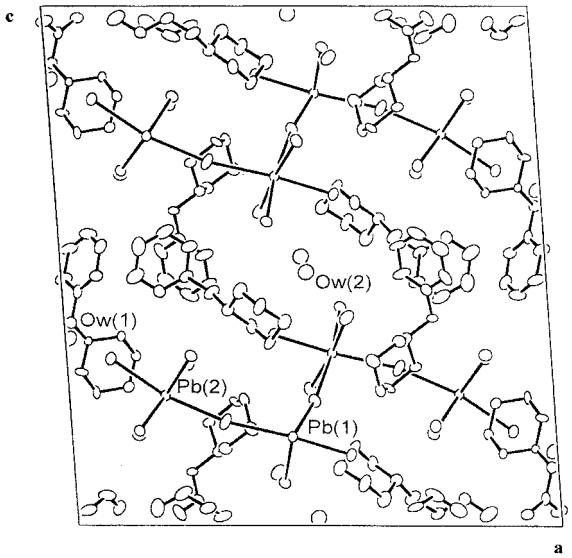

Figure 7. Projection of the structure of $(benzpipzH_2)_3[Pb_2Br_{10}]\cdot 2H_2O$ (**4**) along the *y* direction with vibrational ellipsoids at the 50% probability level.

6 and 7, Table 4). The inorganic ribbons are composed of alternate dinuclear $[Pb_2Br_{10}^{6-}]$ units in which two crystallographically independent lead atoms are present. In each dimer the Pb(1) atom is connected by bridging bromine atoms to two Pb(1) belonging to adjacent dimers. Furthermore, a different bromide atom joins each Pb(2) of the same unit. This gives rise to a polymeric ribbon formed by two zigzag chains running along the *y* axis linked by common edges shared by adjacent octahedra. Coordination around Pb(1) is completed by three bridging and three terminal atoms, while around Pb(2) five terminal bromine atoms, laterally breaking the layers, are present. It is possible to assume that the formation of a dimeric unit, instead of the trimeric one reported elsewhere, is due to the higher steric hindrance of the benzylpiperazinium cation.[3] As shown in Table 4, the Pb−Br distances, ranging from 2.86(3) to 3.05(3) Å for the terminal bromine atoms and from 3.05(3) to 3.20(3) Å for the bridging bromine ones, closely agree with those observed in $(pnH_2)_2[Pb_{1.5}Br_7]\cdot H_2O$.[3] The structure is tied together through a series of hydrogen-bond interactions involving the organic dications, intercalated between the chains, the inorganic ribbons, and the water molecules which contribute

(16) Bonamartini Corradi, A.; Cramarossa, M. R.; Pellacani, G. C.; Battaglia, L. P.; Giusti, J. *Gazzetta Chim. Ital.* **1994**, *124*, 481.

Table 4. Bond Distances (Å) and Angles (deg) with Esd's in Parentheses Involving the Inorganic Moiety of Compound **4**[a]

Pb(1)−Br(11)	2.863	Pb(2)−Br(21)	3.133
Pb(1)−Br(12)	3.238	Pb(2)−Br(22)	2.940
Pb(1)−Br(12)^i	3.147	Pb(2)−Br(23)	3.034
Pb(1)−Br(13)	2.961	Pb(2)−Br(24)	3.053
Pb(1)−Br(14)	2.879	Pb(2)−Br(25)	3.013
Pb(1)−Br(26)	3.202	Pb(2)−Br(26)	3.055
Br(11)−Pb(1)−Br(12)	85.8(1)	Br(21)−Pb(2)−Br(22)	176.1(2)
Br(11)−Pb(1)−Br(12)^i	84.5(1)	Br(21)−Pb(2)−Br(23)	81.8(1)
Br(11)−Pb(1)−Br(13)	89.6(1)	Br(21)−Pb(2)−Br(24)	92.2(1)
Br(11)−Pb(1)−Br(14)	86.5(1)	Br(21)−Pb(2)−Br(25)	93.3(1)
Br(11)−Pb(1)−Br(26)	174.8(1)	Br(21)−Pb(2)−Br(26)	100.4(1)
Br(12)−Pb(1)−Br(12)^i	94.5(1)	Br(22)−Pb(2)−Br(23)	94.4(1)
Br(12)−Pb(1)−Br(13)	84.4(1)	Br(22)−Pb(2)−Br(24)	87.2(1)
Br(12)−Pb(1)−Br(14)	172.1(1)	Br(22)−Pb(2)−Br(25)	90.5(1)
Br(12)−Pb(1)−Br(26)	99.3(1)	Br(22)−Pb(2)−Br(26)	80.1(1)
Br(13)−Pb(1)−Br(12)^i	174.0(1)	Br(23)−Pb(2)−Br(24)	91.8(1)
Br(13)−Pb(1)−Br(14)	93.8(1)	Br(23)−Pb(2)−Br(25)	175.1(1)
Br(13)−Pb(1)−Br(26)	89.9(1)	Br(23)−Pb(2)−Br(26)	87.1(1)
Br(14)−Pb(1)−Br(12)^i	86.4(1)	Br(24)−Pb(2)−Br(25)	88.1(1)
Br(14)−Pb(1)−Br(26)	88.4(1)	Br(24)−Pb(2)−Br(26)	167.1(1)
Br(26)−Pb(1)−Br(12)^i	96.1(1)	Br(25)−Pb(2)−Br(26)	94.0(1)
Pb(1)−Br(26)−Pb(2)	169.1(1)		

[a] i = $1 - x$, $1/2 + y$, $1/2 - z$.

to the crystal packing. As previously observed for other haloplumbates, the presence of uncoordinated water molecules forming hydrogen-bond interactions with terminal bromine atoms [N(14)···Br(11) (*x*, *y*, *z*) 3.33(1) Å, N(14)···Br(23) ($1 - x$, $y - 1/2$, $1/2 - z$) 3.32(2) Å, N(11)···Br(13) ($1 - x$, $1/2 + y$, $1/2 - z$) 3.32(1) Å, N(31)···Br(22) (*x*, *y*, *z*) 3.26(2) Å, N(34)···Br(12) (*x*, *y*, *z*) 3.66(2) Å, N(34)···O(2) (*x*, *y*, *z*) 2.91(3) Å, N(21)···O(1) ($1 - x$, $1/2 + y$, $1/2 - z$) 2.80(2) Å, N(24)···Br(25) ($1 - x$, $1/2 + y$, $1/2 - z$) 3.25(2) Å, N(24)···Br(21) ($1 - x$, $y - 1/2$, $1/2 - z$) 3.33(2) Å] influences the formation of this unusual structural motif, suggesting that the haloplumbate(II) ribbons are not self-consistent and require strong stabilizing crystal packing interactions. Lastly, Pb(1)···Pb(1) ($1 - x$, $y - 1/2$, $z - 1/2$), Pb(1)···Pb(2)($1 - x$, $y - 1/2$, $1/2 + z$), and Pb(1)···Pb(2) contacts are 6.352(4), 8.904(4), and 6.229(3) Å, respectively.

Thermal Results. All the synthesized compounds, investigated by thermogravimetric (TG) and differential scanning calorimetric (DSC) techniques, exhibit no structural phase transition from room temperature up to their melting point (500−560 K) in agreement with the thermal behavior of other haloplumbates presenting similar structural archetypes.[2,3] As previously observed for $(2meptH_2)[Pb_{1.5}I_5]$, the anhydrous complexes under study show, at temperatures several degrees below their respective melting point, a slight and gradual weight loss (<1%) possibly associated with the emission of the correspondent halide acids adsorbed on the crystals.

Measurements carried out on $(me_2pipzH_2)_2[Pb_3I_{10}]\cdot 4H_2O$ and $(benzpipzH_2)_3[Pb_2Br_{10}]\cdot 2H_2O$ compounds reveal a weight loss of 3.3% for the former and 2.0% for the latter, corresponding to the loss of four and two water molecules, respectively, in the temperature range 80−120 °C. From DSC measurements the loss of the water moieties corresponds, in the same temperature range, to an endothermic event and is confirmed by the experimental heat of transformation ($\Delta H = 188.4$ kJ/mol for the dimethylpiperazinium compound and $\Delta H = 95.2$ kJ/mol for the benzylpiperazinium one) four and two times, respectively, greater than the theoretical value found for the dehydration heat of one water molecule in hydrated crystals ($\Delta H = 54-59$ kJ/mol).[17,18]

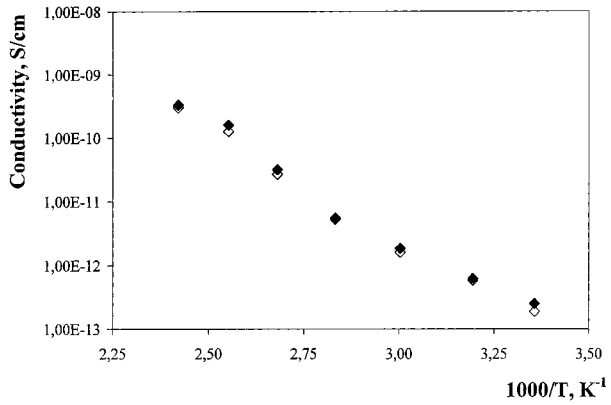

Figure 8. Electrical conductivity, σ, as a function of reciprocal absolute temperature, at 1 (solid symbols) and 60 (open symbols) minutes after voltage application for $(me_2pipzH_2)[PbBr_4]$ (**2**).

Electrical Results. The electrical behavior of all the hydrated **3** and **4** compounds has not been explored, since the loss of water moieties with increasing temperature causes unknown structural changes. Figure 8 shows the electrical conductivity σ of $(me_2pipzH_2)[PbBr_4]$ calculated at 1 and 60 min after the application of the step voltage, in dry nitrogen, as a function of reciprocal absolute temperature in the temperature range 283−500 K. The $(pipzH_2)[PbCl_4]$ compound plot has not been reported since it shows a behavior comparable to the dimethylpiperazinium one. Measurements were performed from the highest allowed temperature to room temperature; transient phenomena, as a function of time, are almost absent, and at higher temperatures a degradation event takes place. Conductivity values range from those typical of insulating materials, at low temperatures, to those of semiconductors at the highest ones. The use of different types of electrodes (Au, C) gave no meaningful variations on the values of conductivity and slope in the log σ versus 1000/T plot. Dielectric measurements in the frequency range $70-10^5$ Hz at different temperatures showed no remarkable relaxation effects. The relative dielectric constant (not shown for the sake of brevity) increases with temperature and regularly decreases with frequency at all the investigated temperatures, reaching at the higher frequencies a value of about 10 at all temperatures. However, the loss factor for the considered compound at constant temperature increases with decreasing frequency (Figure 9).

On account of the exhibited electrical behavior, it therefore seems reasonable to ascribe, as for other previously investigated bidimensional haloplumbates(II) and halocadmates(II), the source of the dc conductivity to proton migration via the hydrogen bonds involving halogen atoms of adjacent polymeric layers and nitrogen atoms of the organic cations.[3,12,19,20] As noted by comparing the electrical conductivity of $(me_2pipzH_2)[PbBr_4]$ with perovskite-like compounds reported elsewhere, conductivity tends to decrease as the distance between the layers decreases.[3] It is also noticeable that haloplumbate(II) compounds presents generally higher values of conductivity compared to the analogous halocadmates(II).

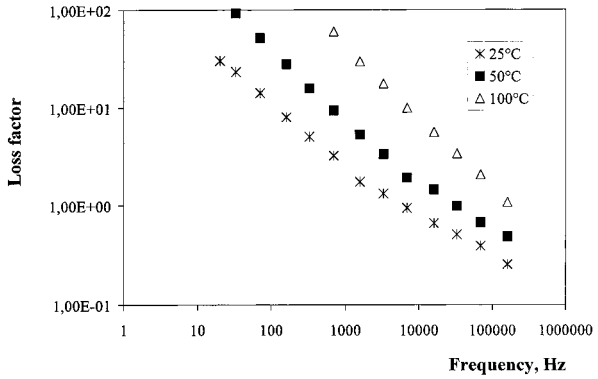

Figure 9. Loss factor, e, as a function of frequency for the $(me_2pipzH_2)[PbBr_4]$ (**2**) compound.

Conclusions

This survey reveals a rich variety of structural model systems including strictly monodimensional, ribbonlike and two-dimensional, layered structures, which result from a diverse range of hydrogen-bond interactions. As observed for other haloplumbate(II) complexes, of particular interest is the observation that chemically similar counterions can produce dramatic changes in the structures.[3] Despite the fact that the organic cations could be remote or not from the coordination center, this diversity occurs as a result of the ability of halide ions to bridge lead atoms and, when present, of the capability of the water moieties to form hydrogen bonds. The whole electrical behavior of the synthesized haloplumbate(II) compounds indicates an ionic type of conduction, generally higher than the correspondent halocadmates(II), due to a mechanism of migration of the protons involved in hydrogen bonds.[21] The electrical conductivity seems to be also related to the distance between the inorganic anions where a closer packing of the structure tends to oppose the ionic mechanism of conduction as noticed for the investigated compounds in comparison with other bidimensional haloplumbates.[3]

Supporting Information Available: Listings of anisotropic thermal parameters for $(pipzH_2)[PbCl_4]$ (**1**) (Table S1), $(me_2pipzH_2)[PbBr_4]$ (**2**) (Table S2), $(me_2pipzH_2)_2[Pb_3I_{10}]\cdot 4H_2O$ (**3**) (Table S3), $(benzpipzH_2)_3[Pb_2Br_{10}]\cdot 2H_2O$ (**4**) (Table S4), fractional atomic coordinates and equivalent isotropic thermal parameters for all the cited compounds (Table S5−S8) and data collection and refinement parameters (Table S9). This material is available free of charge via the Internet at http://pubs.acs.org.

IC000319K

(17) Dei, L.; Guarini G. G. T.; Piccinini, S. *J. Therm. Anal.* **1984**, *29*, 755.
(18) Giusti, J.; Guarini, G. G. T.; Menabue, L.; Pellacani, G. C. *J. Therm. Anal.* **1984**, *29*, 639.
(19) Bonamartini Corradi, A.; Cramarossa, M. R.; Saladini, M.; Giusti, J.; Saccani, A.; Sandrolini, F. *Inorg. Chim. Acta* **1995**, *233*, 85.
(20) Manfredini, T.; Pellacani, G. C.; Battaglia, L. P.; Bonamartini Corradi, A.; Motori, A.; Sandrolini, F. *Mater. Chem. Phys*. **1988**, *20*, 215.
(21) Battaglia, L. P.; Bonamartini Corradi, A.; Pelosi, G.; Cramarossa, M. R.; Manfredini, T.; Pellacani, G. C.; Motori, A.; Saccani, A.; Sandrolini, F.; Giusri, J. *Mater. Eng.* **1989**, *1*, 537.